LAWRENCE
LIVERMORE
NATIONAL
LABORATORY

LLNL-PROC-407244

Advances in understanding the anomalous dispersion of plasmas in the X-ray regime

Joseph Nilsen, K. T. Cheng, Walter R. Johnson

September 25, 2008

11th International Conference on X-ray Lasers
Belfast, United Kingdom
August 17, 2008 through August 22, 2008

Disclaimer

Advances in understanding the anomalous dispersion of plasmas in the X-ray regime

Joseph Nilsen and K. T. Cheng

Lawrence Livermore National Laboratory, Livermore, CA 94551

Walter R. Johnson

University of Notre Dame, Notre Dame, IN 46556

Summary. Over the last several years we have predicted and observed plasmas with an index of refraction greater than one in the soft X-ray regime. These plasmas are usually a few times ionized and have ranged from low-Z carbon plasmas to mid-Z tin plasmas. Our main computational tool has been the average atom code AVATOMKG that enables us to calculate the index of refraction for any plasma at any wavelength. In the last year we have improved this code to take into account many-atomic collisions. This allows the code to converge better at low frequencies.

In this paper we present our search for plasmas with strong anomalous dispersion that could be used in X-ray laser interferometer experiments to help understand this phenomena. We discuss the calculations of anomalous dispersion in Na vapor and Ne plasmas near 47 nm where we predict large effects. We also discuss higher Z plasmas such as Ce and Yb plasmas that look very interesting near 47 nm. With the advent of the FLASH X-ray free electron laser in Germany and the LCLS X-FEL coming online at Stanford in another year we use the average atom code to explore plasmas at higher X-ray energy to identify potential experiments for the future. In particular we look near the K shell lines of near solid carbon plasmas and predict strong effects. During the next decade X-ray free electron lasers and other X-ray sources will be available to probe a wider variety of plasmas at higher densities and shorter wavelengths so understanding the index of refraction in plasmas will be even more essential.

1 Introduction

Since the earliest days of lasers, optical interferometers have been used to measure the electron density of plasmas [1] using the assumption that the index of refraction of the plasma is due only to the free electrons and is therefore less than one [1-2]. With this assumption the electron density of the plasma is directly proportional to the number of fringe shifts in the interferometer. Over the last decade many interferometers [3-8] have been built in the soft X-ray wavelength range of 14 to 72 nm (89 to 17 eV). The experiments done with these sources all assume that only the free electrons contribute to the index of refraction. In the next few years, interferometers will be built using the X-ray free electron lasers, which will extend lasers to even shorter wavelengths [9].

In the last several years interferometer experiments [4-6] of Al plasmas, Ag and Sn plasmas [10], and C plasmas [11-12] observed fringe lines bend in the opposite direction than was expected, indicating that the index of refraction was greater than one. Analysis of the experiments showed that the anomalous dispersion from the resonance lines and absorption edges of the bound electrons have a larger contribution to the index of refraction with the opposite sign as the free electrons [12-15]. Since the original analysis [13] of the experiments with Al plasmas we have developed a new tool AVATOMKG [16] that enables us to calculate the index of refraction for any plasma at any wavelength. This tool is a modified version of the INFERNO average atom code [17] that has been used for many years to calculate the absorption coefficients for plasmas.

In this work we search for other materials that can be used to create plasmas with index of refraction greater than one at X-ray laser energies. We discuss how neutral Na vapor and singly-ionized Ne plasma look to be promising candidates to use in interferometer experiments based on the Ne-like Ar X-ray laser [18] at 26.44 eV or 47 nm. We also discuss higher Z plasmas such as Ce and Yb plasmas, which look very interesting near 47 nm. With the advent of the FLASH X-ray free electron laser in Germany and the LCLS X-FEL coming online at Stanford soon we look at the K shell lines of near solid carbon plasmas and predict strong effects.

2 Analysis of interferometer experiments

When the electron density is much less than the critical density, as is typical for laser produced plasmas, the traditional formula for the index of refraction of a plasma due only to free electrons is approximated as $n = 1 - (N_{elec} / 2N_{crit})$ where N_{elec} is the electron density of the plasma and N_{crit} is the plasma critical density. For a uniform plasma of length L the number of fringe shifts observed in an interferometer equals $(1 - n) L / \lambda$ or $(N_{elec} L) / (2 \lambda N_{crit})$. For a non-uniform plasma one does a path length integral. The fringe shifts are referenced against a set of reference fringes in the absence of any plasma and the formula assumes that the interferometer is in a vacuum. When analyzing an experiment one counts how far the fringes have shifted compared with the reference fringes taken with no plasma and converts this into electron density. For the 46.9 nm Ne-like Ar X-ray laser the number of fringe shifts in the interferometer is $(N_{elec} L) / (4.8 \times 10^{18}\ cm^{-2})$ and the critical density is $5.07 \times 10^{23}\ cm^{-3}$.

To understand the contribution of the bound electrons we look at the relationship between the absorption coefficient and the index of refraction. The total absorption coefficient $\alpha = N_{ion} \sigma = (4 \pi \beta) / \lambda$ where N_{ion} is the ion density of the plasma, λ is the wavelength, σ is the absorption cross-section, β is the imaginary part of the complex index of refraction n* defined by $n^* = 1 - \delta - i\beta$. The real part of the index of refraction $n = 1 - \delta$. The Henke tables [19] tabulate the dimensional-less optical constants f_2 and f_1 for neutral materials. These coefficients are related to δ and β by $\delta = f_1 N_{ion} / (2 N_{crit})$ and $\beta = f_2 N_{ion} / (2 N_{crit})$. From the total absorption cross-section σ we determine the optical constant f_2. We then derive the optical constant f_1 as a function of photon energy E using the Kramers-Kronig dispersion relation [20] by taking the principal value of the integral

$$f_1(E) = Z_{nuc} + \frac{2}{\pi} P.V. \int_0^\infty \frac{f_2(\varepsilon)\, \varepsilon\, d\varepsilon}{E^2 - \varepsilon^2}$$

where Z_{nuc} is the atomic number of the element. For neutral materials the oscillator sum rules insure that f_1 goes to zero at zero energy and Z_{nuc} at infinite energy. For an ionized plasma with average ionization Z* then $f_1 = Z^*$ at $E = 0$.

In the absence of any bound electrons f_1 is equivalent to the number of free electrons per ion. This means that we can replace N_{elec} with $f_1 N_{ion}$ in the formula for the number of fringe shifts. The free electron approximation for the index of refraction is true when f_1 is equal to Z*.

The number of fringe shifts observed in the experiment for a real plasma is now equals (f_1 N_{ion} L) / (2 λ N_{crit}). Taking the ratio of f_1 to Z* gives the ratio of the measured electron density to the actual electron density. When the ratio is negative, the index of refraction is greater than one and the fringes bend the opposite direction than expected in the interferometer.

3 Finding Anomalous Dispersion in Ne and Na Plasmas

For the interferometer that uses the Ne-like Ar X-ray laser at 46.9 nm (26.44 eV) we begin our search for plasmas that might have a large anomalous dispersion near 26.44 eV by first looking at the Henke data to find materials with absorption edges in the 20 – 30 eV range. Since Ne and Na both looked like interesting materials with L shell edges at 21.6 and 30.6 eV, respectively, we extrapolated the Henke data to estimate the f_1 versus photon energy for neutral Ne and Na. Finding negative f_1 values for neutral materials is usually a good clue to find negative f_1 in plasma that are only a few times ionized.

Neutral Ne plasma is very opaque to the 26.44 eV X-rays since they are above the L-shell absorption edge at 21.6 eV. However for single ionized Ne the L-edge moves to 41 eV and the plasma becomes much more transparent. Using an ion density of 10^{20} cm^{-3} at a temperature of 4 eV the average atom code calculates a Z* = 1.05, which is close to singly-ionized. Figure 1 shows the optical constant f_1 versus photon energy for the Ne plasmas. For the case Z* = 0, shown by the dotted line, the Henke data has been extrapolated to lower energy. At an energy of 26.44 eV f_1 = -1.4 for the neutral Ne but this case would be highly absorbing. For the singly ionized case with Z* = 1.05, shown by the solid line, f_1 is now –4.4 at the photon energy of 26.44 eV. This is due to being on the low energy side of the strong 2s – 2p absorption line, which is shifted by +4.18 eV in the calculation so that the line agrees with the experimentally measured value of 26.86 eV [21]. While not shown in the figure, as one continues to ionize Ne to doubly-ionized the strong 2s-2p line moves to lower energy at 25.33 eV and the net result is f_1 reaches a positive value of 3.9 at the 26.44 eV photon energy. In a real experiment using the Ar X-ray laser one could observe the neutral Ne gas go from opaque to transparent as the gas is ionized and furthermore watch the fringe shifts go from negative to positive as Ne is ionized from singly to doubly ionized. At some point there would be no fringe shift when there was the right mixture of singly and doubly ionized Ne.

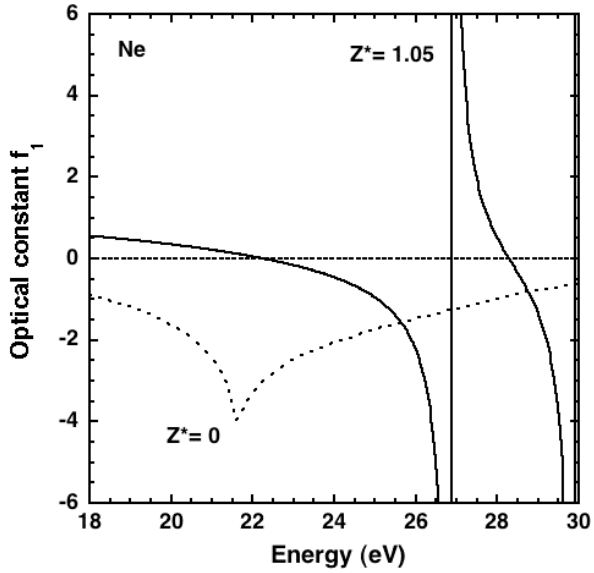

Fig. 1. Optical constant f_1 versus photon energy for Ne plasmas. The dotted line is from the Henke data. The solid curve is calculated by AVATOMKG code for Z* = 1.05. The dashed line is a visual aid for $f_1 = 0$.

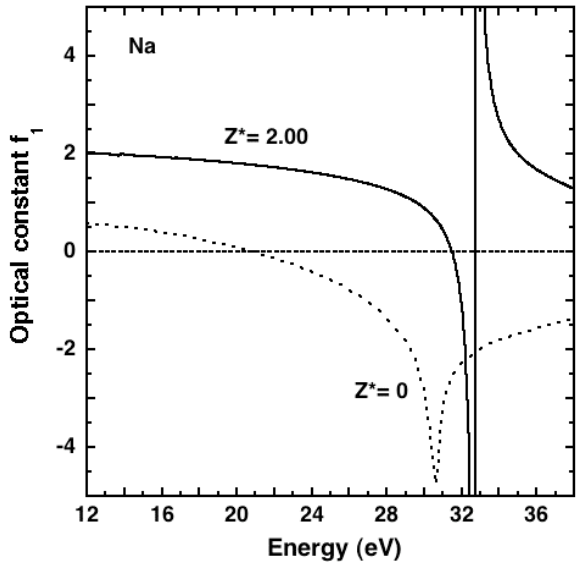

Fig. 2. Optical constant f_1 versus photon energy for Na plasmas. The dotted line is from the Henke data. The solid curve is calculated by AVATOMKG code for Z* = 2.0. The dashed line is a visual aid for $f_1 = 0$.

One could even envision using the ionization state of Ne as a switch that could move the Ar X-ray laser from one direction to another.

Na has a simpler situation than Ne because neutral Na has its L-edge at 30.6 eV and this moves to higher energy as Na is ionized so Na is transparent to the Ar X-ray laser photons for neutral as well as partially ionized ions. The doubly ionized case has the spectrum shifted by 5.5 eV so that the 2s-2p line agrees with the experimentally measured value of 32.7 eV [22]. Figure 2 plots the optical constant f_1 versus photon energy for the two cases with Z* = 0 (Henke data) and Z* = 2.0 (average atom code with temperature of 7.3 eV). This yields f_1 = -0.87 for neutral Na and 1.44 for doubly-ionized Na at 26.44 eV. For singly ionized case the average atom code estimates a value of –0.15 for f_1 at this energy. This suggests that an experiment with neutral Na gas would observe the anomalous dispersion and the fringe shifts would go through a zero point near singly ionized Na and eventually look quite normal as one approached doubly-ionized Na.

4 Finding Anomalous Dispersion in Ce and Yb Plasmas

In addition to low Z materials such as Ne and Na we looked for higher Z elements that could have anomalous dispersion near 26 eV. Two materials that looked interesting were Ce (Z=58) and Yb (Z=70). For the case of neutral Ce there are strong O-edges [19] for the 5p electrons at 19.8 and 17.0 eV that will move to higher energy as the outer electrons are ionized. In particular Ce^{4+} looked very interesting because it is a closed Xe-like core with closed 5s and 5 p sub-shells. The ionization energies for Ce^{0+} to Ce^{3+} are 5.54, 10.85, 20.198 and 36.758 eV, respectively. To estimate the size of the optical constant f_1 we first used the multi-configuration Dirac-Fock (MCDF) code from Grant [23] to calculate the oscillator strengths of ground state transitions in Ce^{4+}. This resulted in five absorption lines whose wavelengths have been measured and documented by NIST[24]. We adjust the position of the calculated lines to agree with the measured line positions. Using the oscillator strength we calculate a value for the absorption coefficient f_2 and use the Kramers-Kronig dispersion relation to calculate the optical constant f_1, shown in Fig. 3. Also shown is the case for neutral Ce extrapolated from the Henke tables. The dominant transitions are two 5p – 5d lines at 25.672 and 31.046 eV with oscillator strengths of 0.256 and 9.31, respectively, and a 5p-6s line at 30.799 eV with oscillator strength of 0.40 which results in f_1 = -17 at 26.44 eV.

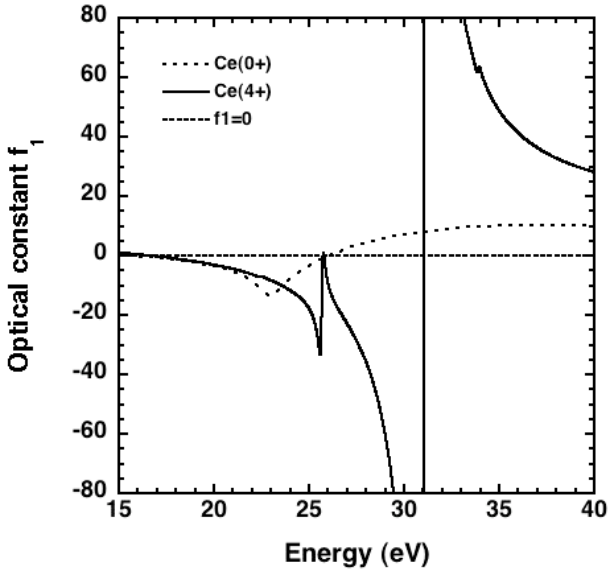

Fig. 3. Optical constant f_1 versus photon energy for Ce plasmas. The dotted line is from the Henke data. The solid curve is calculated for Ce^{4+}. The dashed line is a visual aid for $f_1 = 0$.

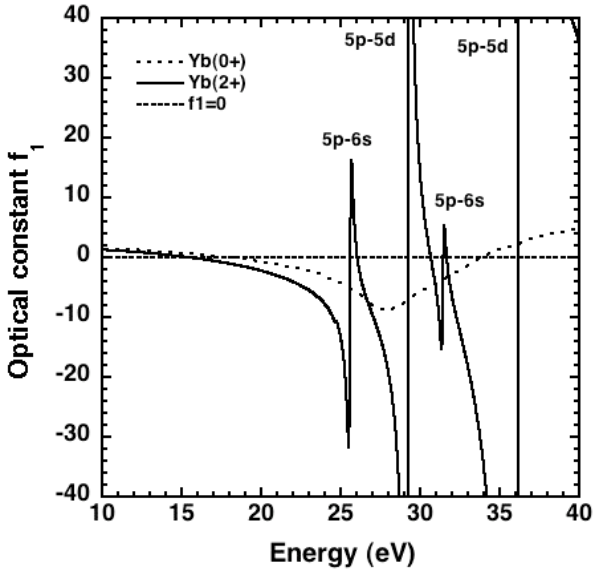

Fig. 4. Optical constant f_1 versus photon energy for Yb plasmas. The dotted line is from the Henke data. The solid curve is calculated for Yb^{2+}. The dashed line is a visual aid for $f_1 = 0$.

In an experiment we would expect to observe an index of refraction larger than one and a large anomalous dispersion.

The second material that looks interesting is Yb. Neutral Yb has O-edges [19] for the 5p electrons at 24.1 and 30.3 eV and an optical constant f_1 = -6.6 at 26.44 eV. As we ionize Yb^{2+} has a completely closed N-shell and closed 5s and 5 p sub-shells. Using the MCDF code to calculate the oscillator strengths of the ground state transitions we predict several strong 5p – 5d lines at 29.2 and 36.1 eV. Using the same procedure described above we then calculate the optical constant f_1 as a function of photon energy, as shown in Fig. 4, for Yb^{2+}. We predict f_1 = -5.2 at 26.44 eV so we would expect an X-ray laser interferometer at 26.44 eV to observe an index of refraction larger than one for this plasma.

5 Modeling of Carbon Plasmas at higher energy

With the advent of the FLASH X-ray free electron laser in Germany and the LCLS X-FEL coming online soon at Stanford we look near the K shell lines of near solid carbon plasmas and predict strong effects near the K-shell absorption edge. We have previously modeled C plasma and predicted and observed strong anomalous effects near 26.44 eV [11,12].
The AVATOMKG code is used to predict the optical constant f_1 versus energy for C at density 0.2 g per cc, temperature of 12 eV, and resulting Z* = 1.91, as shown in Fig. 5. Also shown is the Henke data for neutral C. For the doubly-ionized C one predicts that f_1 is less than zero for energies from 256 to 273 eV, which means that the index of refraction is greater than one over this range and one would observe anomalous effects. With the AVATOMKG code we are prepared to calculate the optical properties of many different plasma over the entire X-ray regime that is available to laboratory X-ray lasers as well as the new X-FEL facilities.

6 Conclusions

For decades the analysis of plasma diagnostics such as interferometers have relied on the approximation that the index of refraction in plasmas is due solely to the free electrons. This makes the index of refraction less than one. Recent X-ray laser interferometer measurements of Al, Sn, Ag, and C plasmas at wavelengths ranging from 13.9 to 46.9 nm observed anomalous results with the index of refraction being greater than one. The

analysis of these plasma show that the anomalous dispersion from both the resonance lines and absorption edges due to the bound electrons can have the dominant contribution to the index of refraction.

To understand how general this anomalous index of refraction effect is we searched for plasmas that should have an index of refraction greater than one in this soft X-ray regime. We present calculations of neutral Na vapor, singly-ionized Ne plasma, Ce^{4+} and Yb^{2+} plasma that predict an index of refraction greater than one at the 46.9 nm (26.44 eV) wavelength of the Ne-like Ar X-ray laser. With the advent of the FLASH X-ray free electron laser in Germany and the LCLS X-FEL at Stanford we look at the K shell lines of near solid carbon plasmas and predict strong anomalous effects with the index of refraction greater than one from 256 to 273 eV.

During the next decade X-ray free electron lasers and other sources will be available to probe a wider variety of plasmas at higher densities and shorter wavelengths so it will be even more essential to understand the index of refraction in plasmas. X-ray laser interferometers may become a valuable tool to measure the index of refraction of plasmas in the future.

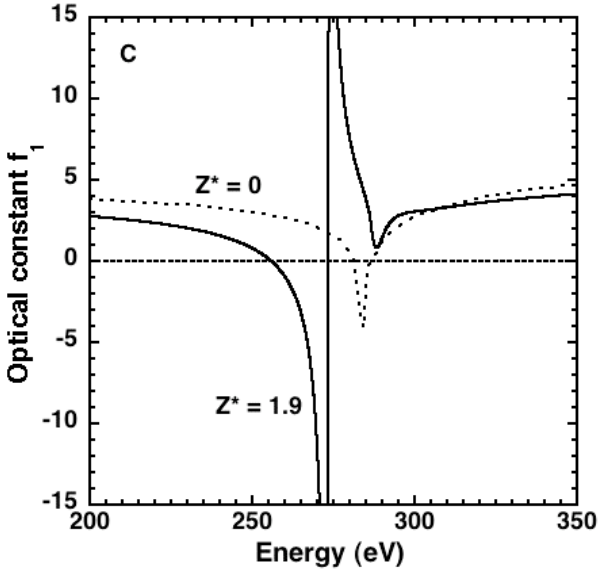

Fig. 5. Optical constant f_1 versus photon energy for C plasmas. The dotted line is from the Henke data. The solid curve is calculated by AVATOMKG code for Z* = 1.9. The dashed line is a visual aid for f1 = 0.

Acknowledgements

Work performed under the auspices of the US Department of Energy by the Lawrence Livermore National Laboratory under Contract DE-AC52-07NA27344. The work of one author (WRJ) was supported in part by NSF Grant No. PHY-0456828.

References

1. G. J. Tallents, J. Phys. D. **17**, 721 (1984).
2. H. R. Griem, *Principles of Plasma Spectroscopy*, (Cambridge University Press, Cambridge, 1997) p. 9
3. L. B. Da Silva et al., Phys. Rev. Lett. **74**, 3991 (1995).
4. H. Tang et al., Appl. Phys. B **78**, 975 (2004).
5. J. Filevich et al., Phys. Rev. Lett. **94**, 035005 (2005).
6. J. Filevich et al., J. Quant. Spectrosc. Radiat. Transfer **99**, 165 – 174 (2006).
7. J. Filevich at al., Opt. Lett **25**, 356 (2000).
8. D. Descamps et al., Opt. Lett. **25**, 135 (2000).
9. A. Meseck et al., Nucl. Inst. And Meth. A **528**, 577 (2004).
10. J. Filevich et al., Phys. Rev. E **74**, 016404 (2006).
11. J. Filevich et al., Laser and Particle Beams **25**, 47 (2007).
12. J. Nilsen et al., "Understanding the anomalous dispersion of doubly-ionized carbon plasmas near 47 nm," HEDP (in press 2008) DOI:10.1016/j.hedp.2008.05.003
13. J. Nilsen and J. H. Scofield, Opt. Lett. **29**, 2677 (2004).
14. J. Nilsen and W. R. Johnson, Applied Optics **44**, 7295 (2005).
15. J. Nilsen, W. R. Johnson, C. A. Iglesias, and J. H. Scofield, J. Quant. Spectrosc. Radiat. Transfer **99**, 425 – 438 (2006).
16. W. R. Johnson, C. Guet, and G. F. Bertsch, J. Quant. Spectrosc. Radiat. Transfer **99**, 327 – 340 (2006).
17. D. A. Liberman, JQSRT **27**, 335 (1982).
18. J. J. Rocca et al., Phys. Rev. Lett. **73**, 2192–2195 (1994).
19. B. L. Henke, E. M. Gullikson, and J. C. Davis, ADNDT **54**, 181 - 342 (1993).
20. L. D. Landau and E. M. Lifshitz, *Electrodynamics of Continuous Media*, (Pergamon, New York, 1984) pp. 280 - 283
21. W. Persson, Phys. Scr. 3, 133 (1971).
22. T. Lundstrom and L. Minnhagen, Phys. Scr. 5, 243 (1972).
23. I. P. Grant et al., Comput. Phys. Commun. **21**, 207 (1980).
24. NIST web site at http://physics.nist.gov/PhysRefData/ASD/index.html